

Conference Paper

Anisotropic Flow Measurements at RHIC

Arkadiy Taranenko

National Research Nuclear University MEPhI, Moscow, 115409, Russia

Abstract

Anisotropic flow measurements in relativistic-heavy ion collisions at RHIC-BNL and LHC-CERN have provided strong evidence for the formation of a strongly coupled Quark-Gluon Plasma (sQGP). In this article, we briefly review and discuss the recent results of anisotropic flow measurements from the STAR and PHENIX experiments at RHIC, such as 1) new measurements at top RHIC energy $\sqrt{s_{NN}}=200$ GeV, 2) collective effects in small and large colliding systems, 3) current results and their understanding from the first beam energy scan program at RHIC (BES-I) and future plans for the BES-II program.

Corresponding Author:

Arkadiy Taranenko
AVTaranenko@mephi.ru

Received: 25 December 2017

Accepted: 2 February 2018

Published: 9 April 2018

Publishing services provided by
Knowledge E

© Arkadiy Taranenko. This article is distributed under the terms of the [Creative Commons Attribution License](#), which permits unrestricted use and redistribution provided that the original author and source are credited.

Selection and Peer-review under the responsibility of the ICPPA Conference Committee.

1. Introduction

The main goal of the experimental heavy ion programs at both the Relativistic Heavy Ion Collider (RHIC) and the Large Hadron Collider (LHC) is to study the transport properties of the strongly interacting matter: the equation of state, the speed of sound, and the value of specific shear viscosity or the ratio of shear viscosity to entropy density (η/s) [1, 2]. The anisotropic flow, as manifested by the anisotropic emission of particles in the plane transverse to the beam direction, is one of the important observables sensitive to these transport properties. The azimuthal anisotropy of produced particles can be quantified by the Fourier coefficients v_n in the expansion of the particles' azimuthal distribution as: $dN/d\phi \propto 1 + \sum_{n=1} 2v_n \cos(n(\phi - \Psi_n))$ [3-5], where n is the order of the harmonic, ϕ is the azimuthal angle of particles of a given type, and Ψ_n is the azimuthal angle of the n th-order event plane. The n th-order flow coefficients v_n can be calculated as $v_n = \langle \cos[n(\phi - \Psi_n)] \rangle$, where the brackets denote an average over particles and events. In this work, we briefly review and discuss the recent results of the measurements of elliptic (v_2) and triangular (v_3) flow at RHIC energies.

2. New results at top RHIC energy

Elliptic (v_2) and triangular (v_3) are the dominant flow signals and have been studied very extensively both at top RHIC and LHC energies. Relativistic viscous hydrodynamics

 OPEN ACCESS

has been successful in describing the observed v_2 and v_3 signals for produced particles in the collisions of heavy-ion systems and the overall good agreement between data and model calculations can be reached for small values of η/s closed to the lower conjectured bound of $1/4\pi$ [1, 2, 6]. In this model framework, the values of the coefficients v_n (for $p_T < 3$ GeV/c) have been attributed to an eccentricity-driven hydrodynamic expansion of the plasma produced in the collision zone. That is, a finite eccentricity moment ϵ_n drives uneven pressure gradients in- and out of the event plane ψ_n , and the resulting expansion leads to the anisotropic flow of particles about this plane. The event-by-event geometric fluctuations in its initial density distribution are found to be responsible for finite elliptic flow signal v_2 in the collisions with almost zero impact parameter, and the presence of odd harmonic moments in the initial geometry ϵ_n and final momentum anisotropy v_n [4, 5]. The event-by event distribution of the hydrodynamic response shows that v_n scales almost linearly with ϵ_n for elliptic (n=2) and triangular (n=3) flow harmonics, with nonlinearities in the response appearing for the harmonics v_4 and higher. The proportionality constant between v_n and ϵ_n is found to be sensitive to the transport properties of the matter such as as the equation of state and the specific shear viscosity η/s . The shear viscosity suppresses higher order harmonic flow coefficients $v_{n>2}$ more strongly than the elliptic flow signal v_2 . The v_n data at top RHIC energies and LHC seem to follow the “acoustic scaling” for anisotropic flow, which suggests that viscous corrections to v_n/ϵ_n grow exponentially as n^2 and $1/(\bar{R}T)$ [7-9]:

$$\frac{v_n(p_T, \text{cent})}{\epsilon_n(\text{cent})} \propto \exp \left[-n^2 \beta' \right], \quad \beta' \propto \frac{\eta}{s} \frac{1}{\bar{R}T} \propto \frac{\eta}{s} \frac{1}{(dN_{ch}/d\eta)^{1/3}} \quad (1)$$

where T is the temperature, \bar{R} is the transverse size of the collision zone and ϵ_n is the n-th order eccentricity moment. For a given harmonic number n, this equation indicates a characteristic linear dependence of $\ln(v_n/\epsilon_n)$ on $1/(\bar{R}T)$, with a slope proportional to η/s [7-9]. The dimensionless size $\bar{R}T$ is approximately proportional to $(dN_{ch}/d\eta)^{1/3}$, where $dN_{ch}/d\eta$ is the charge particle multiplicity density [10]. The data for top RHIC energy show that, for a given centrality, $v_{n>1}$ for all observed hadrons scale to a single curve when plotted as $v_n/n_q^{n/2}$ versus KE_T/n_q , where n_q is the number of constituent quarks in a given hadron species and $KE_T = m_T - m_0$ is the transverse kinetic energy for these hadrons [11, 12].

The observed scaling may indicate that the bulk of the anisotropic flow at top RHIC energies is partonic, rather than hadronic. Lowering the collision energy and studying the energy dependence of anisotropic flow allows a search for the onset of the transition to a phase with partonic degrees of freedom at an early stage of the collision. Figure 1(left) shows the PHENIX results for quark-number (n_q) scaling for v_n of charged

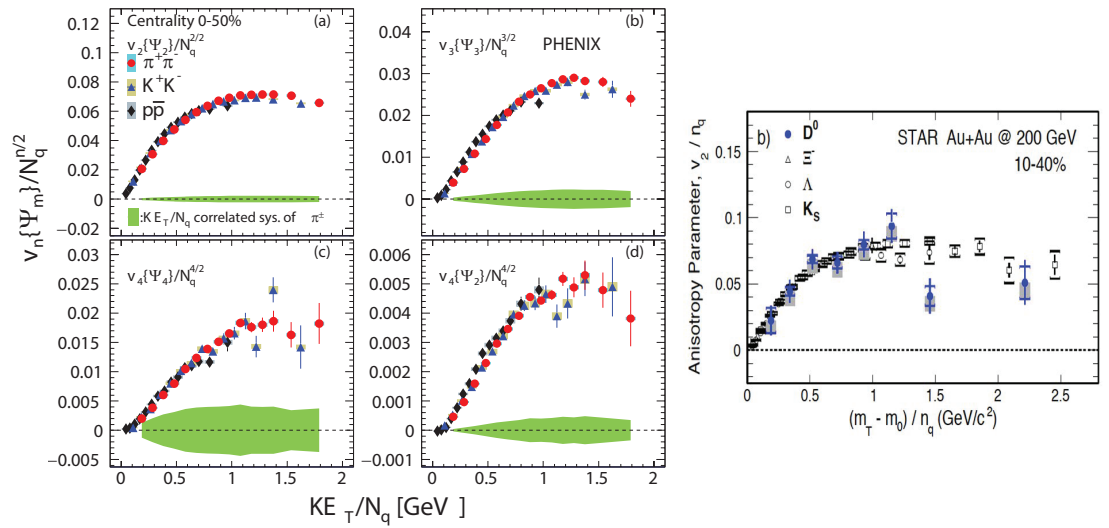


Figure 1: Left: Quark-number (n_q) scaling for 0-50% central Au+Au collisions at $\sqrt{s_{NN}} = 200$ GeV, where n_q is the constituent valence quark number of each hadron and KE_T is the transverse kinetic energy of the hadron [12]. Right: v_2/n_q vs. $(m_T - m_0)/n_q$ for D^0 mesons from 10-40% mid-central Au+Au collisions compared with K_S^0 , Λ , and Ξ^- as measured by STAR [13].

pions, kaons and (anti)protons from 0-50% central Au+Au collisions at $\sqrt{s_{NN}} = 200$ GeV [12]. The right panel of Fig. 1 shows the STAR results for v_2/n_q of D^0 mesons from 10-40% mid-central Au+Au collisions compared with K_S^0 , Λ , and Ξ^- [13]. They show that $D^0 v_2$ follow the same universal trend as all other light hadrons [11, 12]. This may indicate that charm quarks have gained significant flow through interactions with the sQGP medium in 10-40% mid-central Au+Au collisions at $\sqrt{s_{NN}} = 200$ GeV [13].

3. Collective effects in small and large colliding systems

A surprising discovery in high-multiplicity $p+p$ and $p+Pb$ collisions at the LHC and $d+Au$ and ^3He+Au collisions at RHIC was the observation of strong azimuthal anisotropies reminiscent of those in A+A collisions. Namely, an appearance of azimuthal correlations that extend in long-range rapidity known as ridge, mass ordering of the extracted identified particle v_n coefficients, the observation of constituent quark number scaling with transverse kinetic energy and many others (for a comprehensive review we refer to Ref [14, 15]). An outstanding question remains whether the origin of collective effects in small colliding systems can be attributed to hydrodynamic evolution like in heavy-ion collisions or a natural consequence due to initial state dynamics that appear in the final state observables or a combination of both [14]. A promising experiment driven approach for distinguishing the two scenarios is the systematic study of small systems with expected differences in the initial geometry. At top RHIC energy the

different colliding systems such as $p + Au$, $d + Au$ and ${}^3He + Au$ have been analyzed by the PHENIX Collaboration [16]. Due to the nucleon content of the smaller projectile on average one expects a larger elliptic shape in $d + Au$ and a larger triangular shape in ${}^3He + Au$ compared to $p+Au$ collisions.

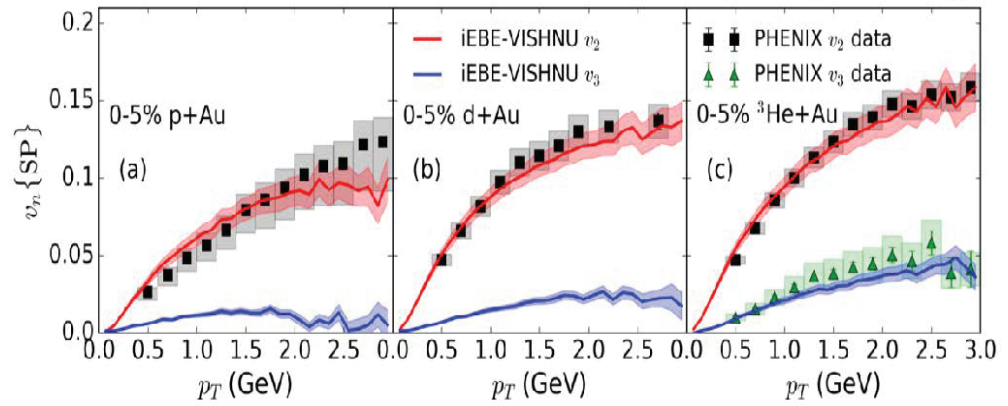


Figure 2: Charged-hadron p_T -differential anisotropic flow coefficients, v_2 and v_3 , compared with PHENIX measurements [16] for 0-5% ($p, d, {}^3He$) + Au collisions at 200 GeV. The figure is taken from [17]

Figure 2 shows the PHENIX results [16] for elliptic v_2 and triangular v_3 event anisotropy measurements in high multiplicity 0-5% most central events in these small collision systems at 200 GeV. The results are remarkably well reproduced by hydrodynamical models [17], which predict a larger elliptic flow in $d + Au$ collision, and triangular flow in ${}^3He + Au$ collisions. Initial state frameworks have yet to perform such a systematic comparison across various collision systems [14]. Figure 3 shows that the azimuthal anisotropy in small systems at RHIC follows the same scaling relations, observed for heavy-ion systems. Namely, the constituent quark number scaling (left panel) and the “acoustic scaling”(right panel). The recent preliminary data from STAR collaboration indicate that v_2/ϵ_2 versus $(N_{ch})^{-1/3}$ has the same slope for charged hadrons from six different colliding systems: U+U, Au+Au, Cu+Au, Cu+Cu, d+Au and p+Au collisions at top RHIC energy [18]. According to the “acoustic scaling” the value of this slope is proportional to η/s . The validation of the scaling relations for so many different colliding systems strongly support the hydrodynamic picture and may indicate that the value of η/s is very similar for different systems. A similar conclusion for the origin of azimuthal anisotropy v_2 and v_3 of charged hadrons from p+p, p+Pb and Pb+Pb collisions at $\sqrt{s} = 5.2$ TeV has been observed in the hybrid viscous hydrodynamical calculations [19]. Using a generalization of the Monte-Carlo Glauber model where each nucleon is a form of three constituent quarks, the model describes very well the experimental v_n data for using a single choice for the transport parameters, such as shear and bulk viscosities [19].

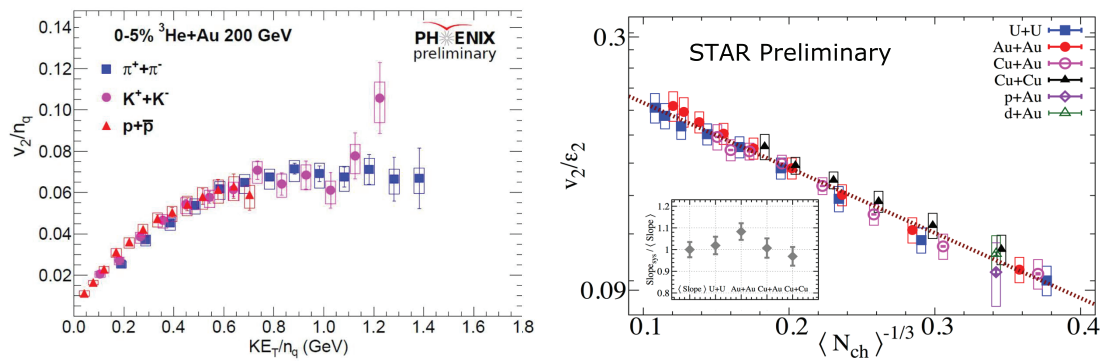


Figure 3: Left: Quark-number (n_q) scaling for 0-5% central ${}^3\text{He} + \text{Au}$ collisions at $\sqrt{s_{\text{NN}}} = 200$ GeV, where n_q is the constituent valence quark number of each hadron and KE_T is the transverse kinetic energy of the charged pions, kaons and (anti)protons measured by PHENIX Collaboration. Right: v_2/ϵ_2 versus $\langle N_{\text{ch}} \rangle^{-1/3}$ for charged hadrons from U+U, Au+Au, Cu+Au, Cu+Cu, d+Au and p+Au collisions at top RHIC energy. The picture with preliminary STAR data was taken from [18].

4. Results from the RHIC BES-I program

The first phase of the Beam Energy Scan (BES-I) program at the Relativistic Heavy Ion Collider (RHIC) is based on Au+Au collision data collected between 2010 and 2014 at center-of-mass energies $\sqrt{s_{\text{NN}}} = 7.7, 11.5, 14.5, 19.6, 27,$ and 39 GeV. The BES-I program has four physics goals: search for the turning off of the signatures of the Quark Gluon Plasma (QGP), the search for the possible first-order phase transition between hadronic gas and QGP, the search for the possible critical end point and the study of the transport properties of the strongly interacting matter as a function of the temperature T and baryon chemical potential μ_B [20–22]. Figure 4(left) shows the p_T dependence of v_2 of charged hadrons calculated from the four-particle cumulant method measured for several centralities and for energies ranging from 7.7 GeV up to 2.76 TeV [23]. It is striking how little the elliptic flow signal for inclusive charged hadron changes over such a wide range of energies and initial energy densities: the energy changes by a factor 400 and initial energy density changes by nearly a factor of 10. Figure 4(right) shows quark-number (n_q) scaled elliptic flow, v_2/n_q versus $(m_T - m_0)/n_q$, for identified particles produced in 0-80% central Au+Au collisions at $\sqrt{s_{\text{NN}}} = 7.7-62.4$ GeV as published by STAR collaboration [24]. This work shows that the scaling holds separately for most of the particles and anti-particles withing 10-15%. The ϕ meson may not follow the trend of the other identified hadrons at 7.7 and 11.5 GeV, but more data are needed before any conclusions can be drawn. Hybrid model calculations show that the weak dependence of $v_2(p_T)$ on the beam energy may result from the interplay of the hydrodynamic and hadronic transport phase [26]. The triangular flow v_3 is more sensitive to the viscous damping and might be an ideal observable to probe the formation of a QGP and the pressure gradients in the early plasma phase.

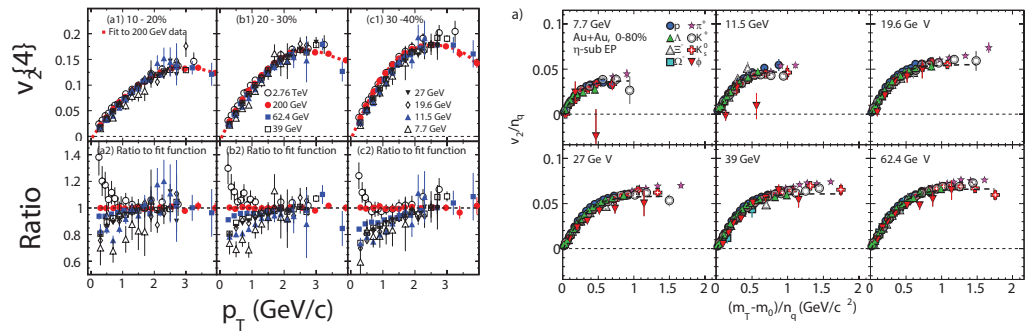


Figure 4: Left: The variation of $v_2\{p_T\}$ for charged hadrons produced at mid-rapidity from 7.7 GeV up to 2.76 TeV [23]. Right: Quark-number (n_q) scaled elliptic flow, v_2/n_q versus $(m_T - m_0)/n_q$, for identified particles produced in 0-80% central Au+Au collisions at $\sqrt{s_{NN}} = 7.7-62.4$ GeV, where n_q is the constituent valence quark number of each hadron and $(m_T - m_0)$ is the transverse kinetic energy of the particle [24].

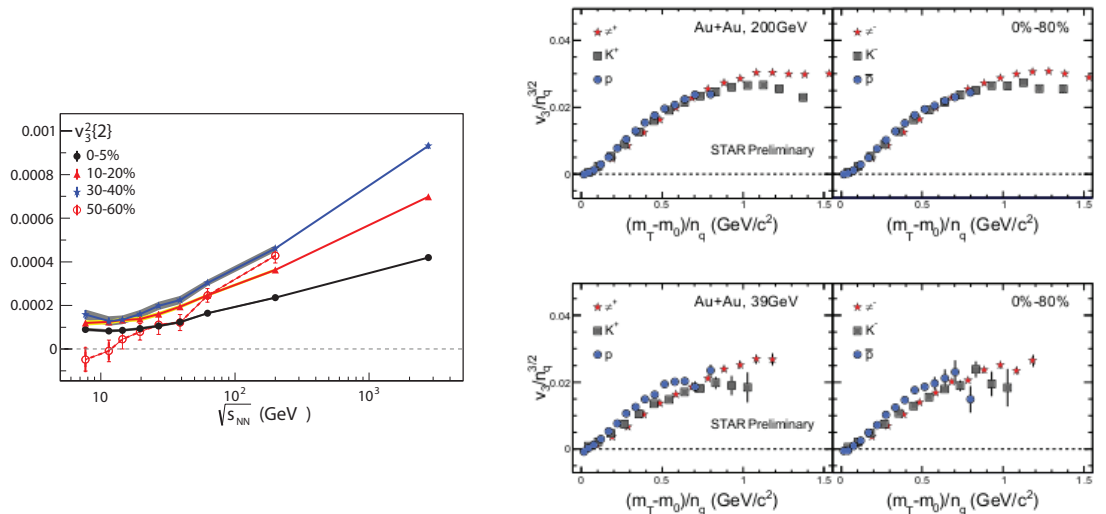


Figure 5: Left: The variation of $v_3^2\{2\}$ for charged hadrons produced at mid-rapidity from 7.7 GeV up to 2.76 TeV [23] for different bins in collision centrality. The figure is taken from [25]. Right: Quark-number (n_q) scaled triangular flow, $v_3/n_q^{3/2}$ versus $(m_T - m_0)/n_q$, for charged pions, kaons and (anti)protons emerged from 0-80% central Au+Au collisions at $\sqrt{s_{NN}} = 200$ GeV (top panels) and at $\sqrt{s_{NN}} = 39$ GeV (bottom panels). The left panels represent the results for particles and right panels for anti-particles. The figure is taken from [27].

Figure 5 left shows the variation of $v_3^2\{2\}$ for charged hadrons produced at mid-rapidity from 7.7 GeV up to 2.76 TeV for different bins in collision centrality [25]. At low energies $\sqrt{s_{NN}} < 14.5$ GeV, the $v_3^2\{2\}$ become consistent with zero in 50-60% peripheral collisions. This result is consistent with the idea of absence of a low viscosity QGP phase in low energy peripheral collisions [26]. For more central collisions, the values of $v_3^2\{2\}$ are positive and change little from 19.6 GeV to 7.7 GeV. For the energies above 19.6 GeV, the values of $v_3^2\{2\}$ linearly increase with the $\log(\sqrt{s_{NN}})$ for all bins in collision centrality [25]. Figure 5 right shows the preliminary data from STAR collaboration for v_3 of identified charged hadrons from Au+Au collisions at $\sqrt{s_{NN}} = 200$ GeV (upper panels)

and 39 GeV (lower panels) [27]. The left panels represent the results for particles and right panels for anti-particles. For 200 GeV the measured v_3 values follow the $v_3/n_q^{3/2}$ versus $(m_T - m_0)/n_q$ scaling. However, for 39 GeV data one can see that the scaling is not so perfect.

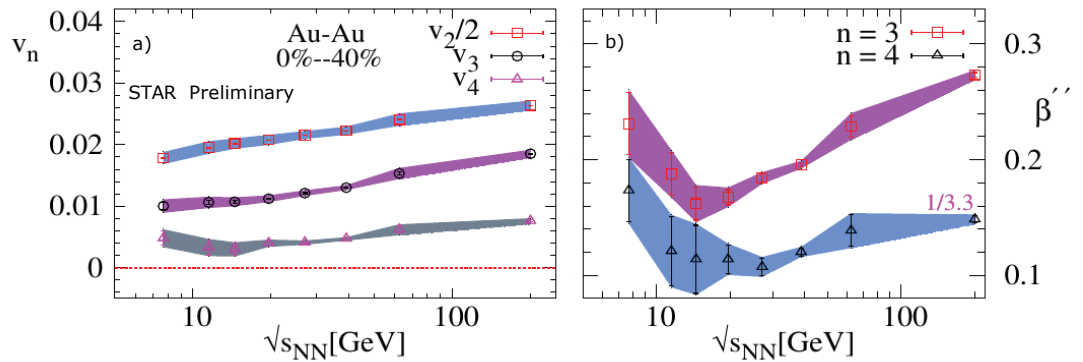


Figure 6: $\sqrt{s_{NN}}$ dependence of the p_T -integrated v_n (left panel) and the estimated viscous coefficient $\beta'' \propto \eta/s$ (right panel). Results are shown for 0-40% central Au+Au collisions; the shaded lines are the systematic uncertainty. The figure is taken from [9].

The left panel of Fig. 6 shows the preliminary STAR data for the $\sqrt{s_{NN}}$ dependence of the p_T integrated v_n of charged hadrons from 0-40% central Au+Au collisions [9]. It shows an essentially monotonic trend for v_2 , v_3 and v_4 with $\sqrt{s_{NN}}$ as might be expected for a temperature increase as $\sqrt{s_{NN}}$ increases [9]. The same authors applied the “acoustic scaling” to v_n data in order to estimate the $\sqrt{s_{NN}}$ dependence of η/s . Using the observation that ϵ_n changes very slowly with beam energy and the measurements for two different harmonics n and n' ($n \neq n'$) the Eq.1 can be simplified [9] to the viscous coefficient $\beta'' \propto (\eta/s) \propto (dN_{ch}/d\eta)^{1/3} \ln(v_n^{1/n}/v_{n'}^{1/n'})$. The right panel of Fig. 6 shows the $\sqrt{s_{NN}}$ dependence of the viscous parameter β'' extracted from the $\ln(v_3^{1/3}/v_2^{1/2})$ and $\ln(v_4^{1/4}/v_2^{1/2})$ results from the left panel of Fig. 6. In contrast to v_n , the excitation function of the viscous parameter β'' shows a non-monotonic behaviour over the same beam energy range. A similar non-monotonic trend for η/s has been observed in the hybrid viscous hydrodynamical calculations [28], tuned to describe the STAR BES-I v_2 data. The next BES-I goal is to search for the predicted first-order phase transition [12, 13] between hadronic and QGP phases. The promising probe which may be sensitive to the pressure produced at early stage is the $v_3^2\{2\}$ signal, please see the previous section. The right panel of Fig. 7 shows $\sqrt{s_{NN}}$ dependence of the $v_3^2\{2\}$ for charged hadrons from Au+Au collisions (data from left panel of Fig. 5) scaled by the charged particle multiplicity per participant pair $n_{ch,PP} = \frac{2}{N_{part}} dN_{ch}/d\eta$ for four bins in collision centrality [25]. The central and semi-central collisions data exhibit a local minimum in the $\sqrt{s_{NN}}$ range around 15-20 GeV which is absent for peripheral collisions.

This is the consequence of a relatively flat trend for $v_3^2\{2\}$ and monotonically increasing trend for the $n_{ch,PP}$ in the energy range $7.7 < \sqrt{s_{NN}} < 20$ GeV. If the general increase of $v_3^2\{2\}$ is driven by ever increasing pressure gradients in ever denser systems at higher energies, then the local minimum in $v_3^2\{2\}/n_{ch,PP}$ could be an indication of an anomalously low pressure inside the matter created in collisions with energies near 15-20 GeV, where a minimum is also observed for the slope of net-proton directed flow [25]. The interpretation of data in this energy regime is complicated by changes in meson to baryon ratio, baryon stopping, non-flow effects and fluctuations, and longer passing time at lower energies [25].

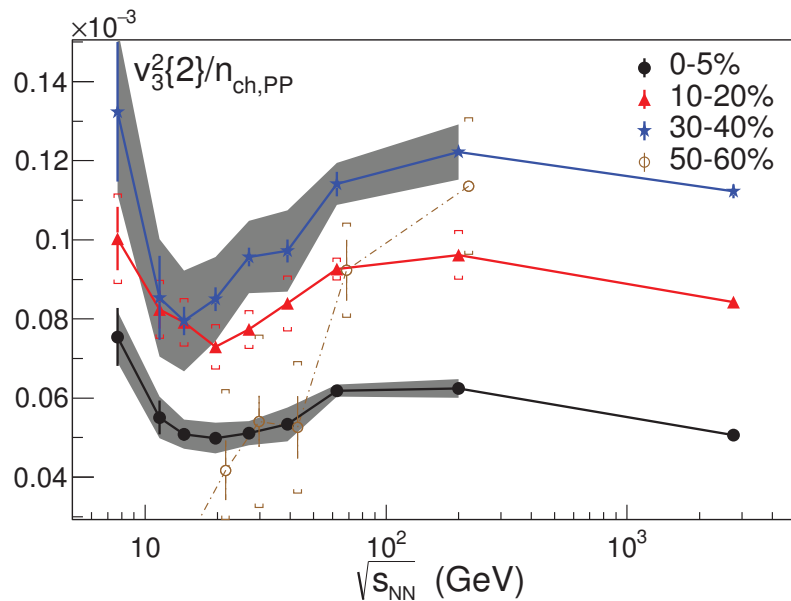


Figure 7: Beam energy dependence of $v_3^2\{2\}$ of charged hadrons divided by the mid-rapidity, charged particle multiplicity, pseudo-rapidity density per participant pair in Au+Au and Pb+Pb (2.76 TeV) collisions. The figure is taken from [25].

The STAR Collaboration has planned a second phase of the Beam Energy Scan program at RHIC (BES-II), scheduled for 2019-2020, to explore the high baryon density region of the QCD phase diagram [29, 30]. The upgrades for STAR detector and RHIC accelerator have been started. The stochastic electron cooling technique and long beam bunches will be applied to accelerate gold beam, which will improve the luminosity by a factor about 10 at $\sqrt{s_{NN}} = 19.6$ GeV to 25 at $\sqrt{s_{NN}} = 7.7$ GeV compared to BES-I. The proposed Fixed-Target program (FXT)[31], which uses only one beam on an internal target will allows STAR to reach higher μ_B ($\mu_B = 720$ MeV for $\sqrt{s_{NN}} = 3$ GeV) with high luminosity. There are three detector upgrades are ongoing at STAR: the iTPC upgrade [32], the Event Plane Detector (EPD) upgrade [33] and the eTOF upgrade [34]. The inner TPC (iTPC) of STAR[32] is being upgraded to improve the energy loss dE/dx resolution, momentum resolution, the pseudo-rapidity acceptance from $|\eta| < 1$ to

$|\eta| < 1.5$ and acceptance for low p_T particles from 125 MeV/c to 60 MeV/c. The EPD is a new dedicated event-plane and centrality detector placed in the forward rapidity region $2 < |\eta| < 4$. With 16 radial segments and 24 azimuthal segments, the detector will provide precise measurements of both the collision centrality and the event plane for all possible harmonics.

Acknowledgments

This work was partially supported by the Ministry of Science and Education of the Russian Federation, grant N 3.3380.2017/4.7, and by the National Research Nuclear University MEPhI in the framework of the Russian Academic Excellence Project (contract No. 02.a03.21.0005, 27.08.2013).

References

- [1] C. Gale, S. Jeon, B. Schenke, P. Tribedy and R. Venugopalan, Phys. Rev. Lett. **110** (2013) no.1, 012302
- [2] U. Heinz and R. Snellings, Ann. Rev. Nucl. Part. Sci. **63** (2013) 123
- [3] S. Voloshin and Y. Zhang, Z. Phys. C **70** (1996) 665
- [4] S. A. Voloshin, A. M. Poskanzer and R. Snellings, arXiv:0809.2949 [nucl-ex].
- [5] R. Snellings, J. Phys. G **41** (2014) no.12, 124007
- [6] R. Derradi de Souza, T. Koide and T. Kodama, Prog. Part. Nucl. Phys. **86** (2016) 35
- [7] R. A. Lacey, A. Taranenko, J. Jia, D. Reynolds, N. N. Ajitanand, J. M. Alexander, Y. Gu and A. Mwai, Phys. Rev. Lett. **112** (2014) no.8, 082302
- [8] R. A. Lacey, D. Reynolds, A. Taranenko, N. N. Ajitanand, J. M. Alexander, F. H. Liu, Y. Gu and A. Mwai, J. Phys. G **43** (2016) no.10, 10LT01
- [9] N. Magdy [STAR Collaboration], J. Phys. Conf. Ser. **779** (2017) no.1, 012060.
- [10] R. A. Lacey *et al.*, arXiv:1601.06001 [nucl-ex].
- [11] R. A. Lacey and A. Taranenko, PoS CFRNC **2006** (2006) 021
- [12] A. Adare *et al.* [PHENIX Collaboration], Phys. Rev. C **93** (2016) no.5, 051902
- [13] L. Adamczyk *et al.* [STAR Collaboration], Phys. Rev. Lett. **118** (2017) no.21, 212301
- [14] B. Schenke, Nucl. Phys. A **967** (2017) 105
- [15] A. Ohlson, Nucl. Phys. A **967** (2017) 97.
- [16] C. Aidala *et al.*, Phys. Rev. C **95** (2017) no.3, 034910
- [17] C. Shen, J. F. Paquet, G. S. Denicol, S. Jeon and C. Gale, Phys. Rev. C **95** (2017) no.1, 014906

- [18] N. Magdy [STAR Collaboration], Talk at AGS/RHIC User meeting 2017
- [19] R. D. Weller and P. Romatschke, Phys. Lett. B **774** (2017) 351
- [20] X. Luo, Nucl. Phys. A **956** (2016) 75
- [21] D. Keane, J. Phys. Conf. Ser. **878** (2017) no.1, 012015.
- [22] H. Caines, Nucl. Phys. A **967** (2017) 121.
- [23] L. Adamczyk *et al.* [STAR Collaboration], Phys. Rev. C **86** (2012) 054908
- [24] L. Adamczyk *et al.* [STAR Collaboration], Phys. Rev. C **88** (2013) 014902
- [25] L. Adamczyk *et al.* [STAR Collaboration], Phys. Rev. Lett. **116** (2016) no.11, 112302
- [26] J. Auvinen and H. Petersen, Phys. Rev. C **88** (2013) no.6, 064908
- [27] X. Sun [STAR Collaboration], J. Phys. Conf. Ser. **535** (2014) 012005.
- [28] I. A. Karpenko, P. Huovinen, H. Petersen and M. Bleicher, Phys. Rev. C **91** (2015) no.6, 064901
- [29] STAR Note 598. <https://drupal.star.bnl.gov/STAR/starnotes/public/sno598>
- [30] C. Yang [STAR Collaboration], Nucl. Phys. A **967** (2017) 800.
- [31] K. Meehan [STAR Collaboration], Nucl. Phys. A **967** (2017) 808
- [32] STAR Note 619. <https://drupal.star.bnl.gov/STAR/starnotes/public/sno619>
- [33] STAR Note 666. <https://drupal.star.bnl.gov/STAR/starnotes/public/sno666>
- [34] [STAR Collaboration and CBM eTOF Group], arXiv:1609.05102 [nucl-ex].